Available online at www.sciencedirect.com

SciVerse ScienceDirect

Ceramics International 39 (2013) S81–S85

CERAMICS INTERNATIONAL

www.elsevier.com/locate/ceramint

High- and low-field dielectric responses and ferroelectric properties of $(Bi_{0.5}Na_{0.5})Zr_{1-x}Ti_xO_3$ ceramics

Panupong Jaiban[a], Sukanda Jiansirisomboon[a,b], Anucha Watcharapasorn[a,b,*], Rattikorn Yimnirun[c], Ruyan Guo[d], Amar S. Bhalla[d]

[a]Department of Physics and Materials Science, Faculty of Science, Chiang Mai University, Chiang Mai 50200, Thailand
[b]Materials Science Research Center, Faculty of Science, Chiang Mai University, Chiang Mai 50200, Thailand
[c]School of Physics, Institute of Science, Suranaree University of Technology, Nakhon Ratchasima 30000, Thailand
[d]Department of Electrical and Computer Engineering, College of Engineering, The University of Texas at San Antonio, TX 78249, San Antonio, USA

Available online 16 October 2012

Abstract

Bismuth sodium zirconate titanate $(Bi_{0.5}Na_{0.5})Zr_{1-x}Ti_xO_3$ with ($x=0$, 0.1, 0.2, 0.3, 0.4, 0.5 and 0.6) ceramics was fabricated by a conventional sintering technique at 850–1000 °C for 2 h. From X-ray diffraction study, three regions of different phases were observed in the ceramic system; i.e., orthorhombic phase region ($0 \le x \le 0.2$), mixed-phase region ($0.3 \le x \le 0.4$), and rhombohedral phase region ($0.5 \le x \le 0.6$). It was observed that the phase evolution from orthorhombic to rhombohedral symmetry resulted in a noticeable increase of the dielectric properties. The results from the high- and low-field dielectric responses indicated that the dielectric properties of both BNZ and BNZT ceramics were dominantly attributed to the reversible contribution. It was also noticed that grain size showed only partial influence on the increase of low-field dielectric constant in Ti-rich BNZT ceramic.

Keywords: C. Dielectric properties; C. Electrical properties; D. Perovskites; BNZT

1. Introduction

To speak of an interesting lead-free novel perovskite materials, bismuth sodium zirconate-based ($Bi_{0.5}Na_{0.5}ZrO_3$; BNZ) ceramic, which had just been reported a few years ago [1,2], is one of those electronic materials. Since it promoted a negative temperature resistance behavior [3], the system was believed to become a promising candidate in lead-free compounds for electronic devices; i.e., sensor, actuator and NTC thermistors. However, electrical properties of BNZ-based materials are scarcely reported. Recently, room temperature dielectric properties of $Bi_{0.5}Na_{0.5}Zr_{1-x}Ti_xO_3$ ceramics (BNZT) with $0.3 \le x \le 0.6$ were reported by Jaiban et al. [4,5]. They found that the relative dielectric constants for these materials were rather low ($\varepsilon_r \approx 170$–$430$). Nevertheless, it should be noted that relatively low values of ε_r measured at low electric field were attributed mainly to a reversible contribution (intrinsic properties from lattice vibration and single-domain responses) [6]. On the contrary, high-field permittivity (differential permittivity) provides information on both the reversible and irreversible contributions (extrinsic domain-switching related property, i.e. domain wall motion) [6]. It is thus our motivation to seek better understanding on low- and high-field dielectric behavior of BNZ and BNZT systems to elucidate the different contributions. In addition, study of the ferroelectric properties of BNZ and BNZT is also scarce. Hence, a purpose of this study is to investigate phase, microstructure, low- and high-field dielectric responses and ferroelectric properties of $Bi_{0.5}Na_{0.5}Zr_{1-x}Ti_xO_3$ ceramics where $x=0$, 0.1, 0.2, 0.3, 0.4, 0.5 and 0.6.

2. Experimental

The specimens were fabricated according to the chemical formula $(Bi_{0.5}Na_{0.5})Zr_{1-x}Ti_xO_3$, where $x=0$, 0.1, 0.2, 0.3,

*Corresponding author at: Department of Physics and Materials Science, Faculty of Science, Chiang Mai University, Chiang Mai 50200, Thailand. Tel.: +66 53 94 1921; fax: +66 53 94 3445.
E-mail address: anucha@stanfordalumni.org (A. Watcharapasorn).

0272-8842/$ - see front matter © 2012 Elsevier Ltd and Techna Group S.r.l. All rights reserved.
http://dx.doi.org/10.1016/j.ceramint.2012.10.039

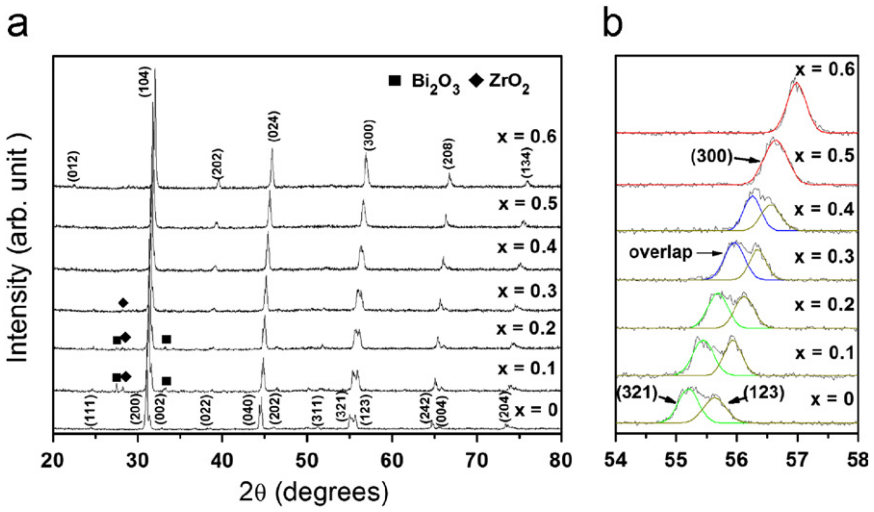

Fig. 1. X-ray diffraction patterns of BNZT ceramics (a) $20 \leq 2\theta \leq 80$ and (b) $54 \leq 2\theta \leq 58$. The data of BNZT ceramics $0.3 \leq x \leq 0.6$ are taken from our previous report [4]. (For interpretation of the references to color in this figure, the reader is referred to the web version of this article.)

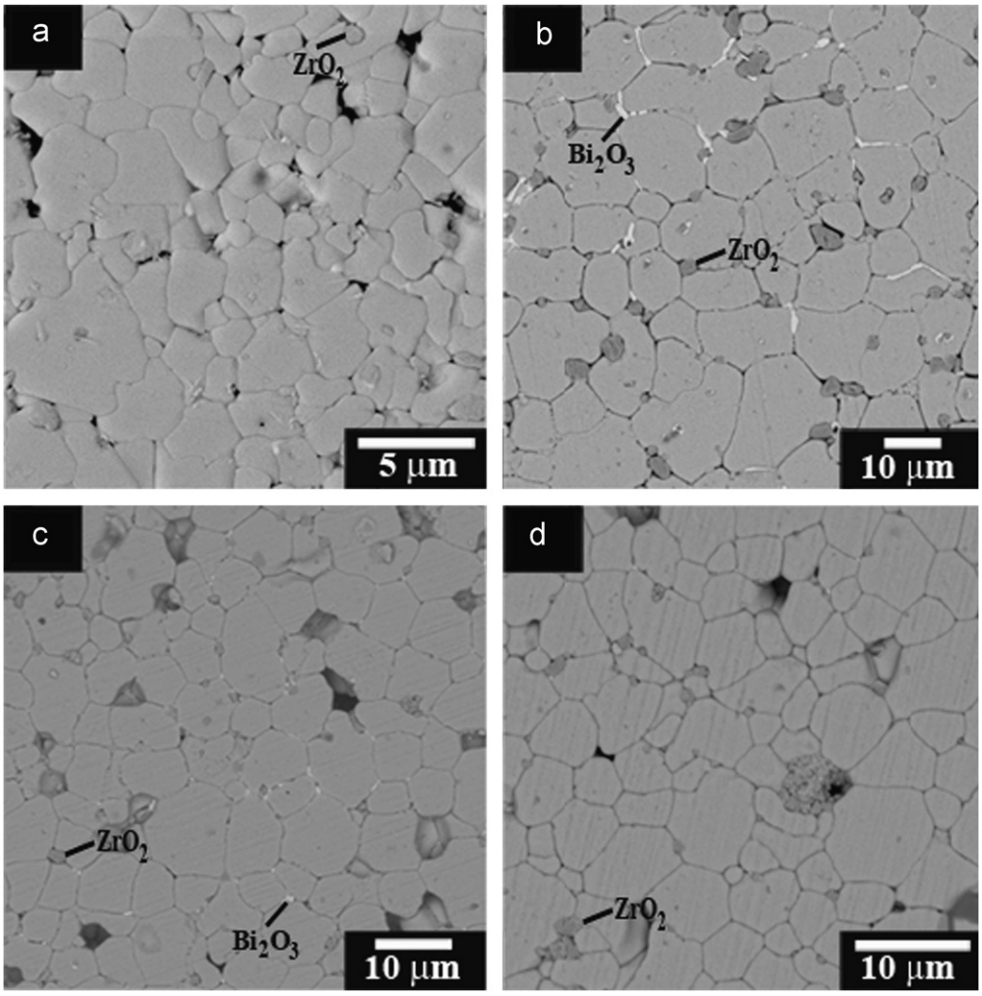

Fig. 2. SEM–BEI images of BNZT ceramics for (a) $x=0$, (b) $x=0.1$, (c) $x=0.5$ and (d) $x=0.6$. The microstructural data for $x=0.5$ and 0.6 are taken from our previous report [4].

0.4, 0.5 and 0.6. The starting materials used in this study were ZrO_2 (99%, Riedel-de Haël]n), TiO_2 (99%, Riedel-de Haël]n), Bi_2O_3 (98%, Fluka) and Na_2CO_3 (99.5%, RdH). The mixtures of oxides were ball milled in ethanol for 24 h. The mixed powders were dried and calcined at 800 °C for 2 h. After sieving, the mixed powder was pressed into

pellets with a diameter of 10 mm using a uniaxial press. These pellets were then sintered at 850–1000 °C for 2 h.

Phase identification of the specimens was investigated in 2θ range of 20–80° using an X-ray diffractometer (XRD, Phillip Model X-pert). A backscattered-electron mode of scanning electron microscope (JSM 6335F) was used to observe microstructure of the selected ceramics. Low-field dielectric permittivity and loss were measured at room temperature with a measured frequency of 1 kHz using 4284 A LCR-meter. Ferroelectric hysteresis loop was obtained using a computer controlled modified Sawyer–Tower circuit. The electric field was applied to a sample by a high voltage AC amplifier at 20 kV. The polarization–electric field (P–E) loop was then recorded by a digital oscilloscope. Differential permittivity (high-field dielectric constant), energy loss, remanent polarization (P_r) and coercive field (E_c) values were then determined from the hysteresis loops. From the P–E loops, the differential permittivity [7] can be calculated approximately by using Eq. (1), which gives

$$\varepsilon = \frac{\Delta P}{\Delta E} \quad (1)$$

where ε=the differential permittivity, ΔE=applied field between +1 and −1 kV/cm, ΔP=polarization difference between +1 and −1 kV/cm.

3. Results and discussion

Phase identification of $Bi_{0.5}Na_{0.5}Zr_{1-x}Ti_xO_3$ ceramics where x=0, 0.1, 0.2, 0.3, 0.4, 0.5 and 0.6 using X-ray diffraction technique in 2θ range between 20–80° is shown in Fig. 1(a). In BNZ pure ceramic, the XRD pattern showed that BNZ ceramic possessed orthorhombic perovskite phase, in good agreement with previously reported literature [1–3]. As Ti addition, shift of diffraction pattern toward a higher reflection angle was seen due to the fact that smaller Ti^{4+} ions (0.605 Å) [8] substituted larger Zr^{4+} ions (0.72 Å) [8] within the lattice to reduce unit cell volume. Moreover, the analysis revealed a non-perovskite peak existence of Bi_2O_3 (JADE no. 054873) for Ti addition of x=0.1 and 0.2, and ZrO_2 (JADE no. 371484) for the Ti addition up to x=0.3. Formation of both un-desired phases would be explained together with their microstructural evidences in SEM study. Based on fitting profile within 2θ range of 54–58° as displayed in Fig. 1(b), a structural transition was found to occur gradually between the orthorhombic, (321) and (123) peaks, and rhombohedral phase, (300) peak. The phases were divided into three regions, the single orthorhombic phase region up to x=0.2 mol fraction, a two-phase region at x=0.3 and 0.4 mol fraction in which (321) orthorhombic and (300) rhombohedral peaks overlapped to cause a left side intensity (blue peak) to become higher than a right side (123 peak), then a single rhombohedral phase region beyond x=0.5 mol fraction.

SEM–BEI micrographs of the selected specimens at composition x=0, 0.1, 0.5 and 0.6 are displayed in Fig. 2. The images revealed an inhomogeneous area of all ceramics although X-ray diffraction technique could not detect these phases within the samples x=0, 0.5 and 0.6. EDX analysis (not shown here) suggested that liquid-like (white) and precipitate-like (dark gray) regions were Bi_2O_3 and ZrO_2 starting phases, respectively. For Bi_2O_3 phase, it was possibly due to sodium deficiency in some areas, which caused an excess Bi_2O_3-like stoichiometry at A-site of the systems during fabrication to induce Bi-rich liquid phase formation. This hypothesis conformed to Pb-rich liquid phase presence as a result of an excess PbO at A-site in PZT ceramic [9,10]. For the existence of ZrO_2 phase, Bi_2O_3 was expected to decompose together with Na_2CO_3 resulting in both Bi and Na A-site deficiency to provide second phase (ZrO_2) precipitates. This observation was also in good agreement with the presence of ZrO_2 phase in a well-known PZT ceramic due to PbO A-site deficiency [9,10]. The influence of these secondary non-perovskite phases and microstructure on BNZT properties will be discussed in later section.

Dielectric properties at high electric field (1 kV/cm) and low electric field (10 V/cm) of the ceramics as a function of Ti content are shown in Fig. 3. The dielectric constant at low field (blue dot line) [4] for compositions of Ti with $0 \le x \le 0.2$ increased only slightly, then increased more rapidly at higher Ti content of $0.3 \le x \le 0.6$. Since, in

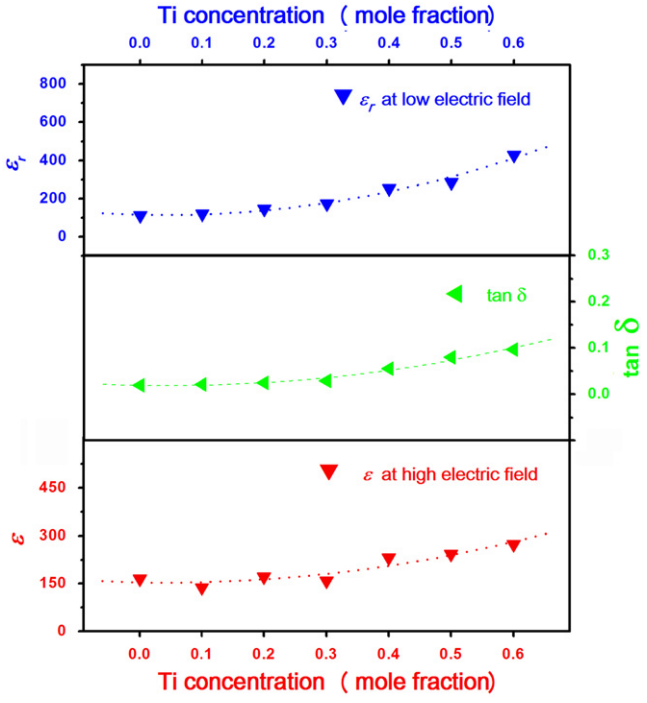

Fig. 3. Plot of the relative permittivity (high and low electric field) and dielectric loss as a function of Ti concentration of BNZT ceramics. The low-field permittivity and dissipation factor of BNZT ceramics $0.3 \le x \le 0.6$ are taken from our previous report [4]. (For interpretation of the references to color in this figure, the reader is referred to the web version of this article.)

general, polarizability of atoms in the rhombohedral lattice is better than in the orthorhombic lattice, resulting in higher relative permittivity [11], the rhombohedral phase transition in the system was expected to be a main factor for an observed increase in the low-field dielectric properties. The dielectric constant enhancement was also accompanied with the increase in the low-field dielectric loss tangent (dissipation factor), as plotted in Fig. 3. The dissipation factor (green dash line) of BNZ and BNZT ceramics measured at room temperature with frequency 1 kHz was seen to change rapidly near the composition with $x=0.3$. The result was clearly in good agreement with dielectric constant tendency. It was basically due to the materials having high dielectric constant also possess higher dielectric loss.

In case of the high-field permittivity (red dot line), it was found that the slope increment was also distinct at $0.3 \leq x \leq 0.6$. The high-field dielectric properties of the BNZ and BNZT ceramics were also due to the phase transition influence. More importantly, it was found that both high- and low-field dielectric permittivity values were not very much different for all compositions. To some extent, this observation may imply that there was only little irreversible contribution (from the domain wall motion) to the dielectric properties of the BNZT ceramic system (within the compositional range of $0 \leq x \leq 0.6$).

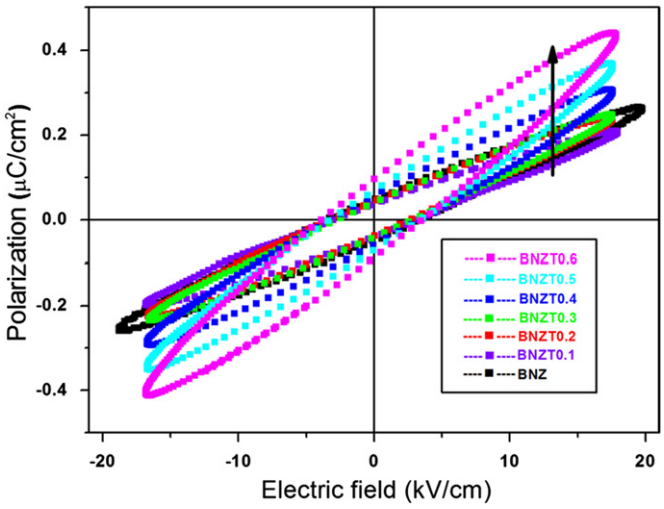

Fig. 4. *P–E* hysteresis loops of BNZT ceramics.

Table 1
Remnant polarization, coercive field, grain size and energy loss of BNZT ceramics.

Ti content	P_r[a] ($\mu C/cm^2$)	E_c[a] (kV/cm)	Grain size (μm)	Energy loss (kJ/m^3)
0	0.04	3.43	1.92 ± 0.73	3.08
0.1	0.04	3.12	6.68 ± 1.66	2.58
0.2	0.04	2.95	6.32 ± 1.26	2.57
0.3	0.04	2.85	5.65 ± 1.63[b]	2.27
0.4	0.07	3.37	5.55 ± 1.84[b]	3.81
0.5	0.06	3.41	5.07 ± 1.57[b]	3.83
0.6	0.09	3.77	3.76 ± 1.24[b]	5.28

[a]Ferroelectric data at room temperature and an electric field of 20 kV/cm.
[b]Data are taken from the previous report [4].

The *P–E* hysteresis loops of BNZ and BNZT ceramics at electric field 20 kV/cm are shown in Fig. 4. It was found that all samples showed some elliptic shape loop. The high dielectric loss of BNZ and BNZT ceramics clearly caused the unsaturated loop because the loss values of these ceramics (0.02–0.10) were rather high as compared to well-known ferroelectric ceramics; i.e., $BaTiO_3$ (0.005–0.01) [12] and $Pb(Zr_{1-x}Ti_x)O_3$ (0.004–0.02) [13] with well documented saturated *P–E* loops. It was therefore difficult to observe saturated loops in these BNZ and BNZT ceramics. Nonetheless, the area of *P–E* loop could indicate the polarization dissipation energy of ferroelectric materials under one full cycle of electric field application [6]. This amount of the energy loss was directly related to the amount of domains participating in the switching process during the application of electric field [6,14]. The calculated hysteresis losses for these ceramics are listed in Table 1. It was observed that the numerical data range of BNZT ceramics was about 2–6 kJ/m^3. The values did not differ significantly. This result further supported that the domain wall movement in these ceramics was rather deficient. This information supported very well the dielectric results at high and low field (Fig. 3). Thus, it could be mentioned that the dielectric response of BNZ and BNZT ceramics at both high- and low-field was mainly attributed to the reversible contribution (intrinsic dielectric property). For remanent polarization and coercive field of BNZ and BNZT (Table 1), it could be seen that the values did not show any significant variation. In addition, it should be mentioned that the non-perovskite phases (discussed earlier in SEM micrographs) did not influence significantly the dielectric and ferroelectric properties of BNZ and BNZT ceramics, which were governed largely by the rhombohedral phase transformation and loss tangent, respectively. As listed in the Table 1, the contribution from different grain size (higher internal stress of smaller grain) could only be noticed to partly influence the low-field dielectric constant enhancement in BNZT ceramic with $x=0.6$ (with grain size of ≈ 3.76 μm), where the dielectric constant value (Fig. 3) was increased about 50% over that of the BNZT ceramic with $x=0.5$ (with larger grain size of ≈ 5.07 μm).

4. Conclusions

In this study, $(Bi_{0.5}Na_{0.5})Zr_{1-x}Ti_xO_3$ ($x=0$, 0.1, 0.2, 0.3, 0.4, 0.5 and 0.6) ceramics were successfully fabricated by a conventional sintering technique. Phase region of the ceramics was divided into three regions: the orthorhombic phase ($0 \leq x \leq 0.2$), the mixed-phase ($0.3 \leq x \leq 0.4$) and the rhombohedral phase ($0.5 \leq x \leq 0.6$). The presence of Bi_2O_3 and ZrO_2 secondary phases did not affect significantly the properties of the ceramics. BNZ and BNZT ceramics showed elliptic-shaped hysteresis loops. The rhombohedral phase transition in Ti-added ceramics could enhance the dielectric properties of BNZ prototype material. From high- and low-field dielectric response analysis,

the dielectric properties of the BNZ and BNZT ceramics were dominated mainly by the reversible contribution. The partial influence of the grain size on the low-field dielectric constant was only observed in Ti-rich BNZT ceramic.

Acknowledgments

This work is financially supported by the Thailand Research Fund (TRF) and the National Research University Project under Thailand's Office of the Higher Education Commission (OHEC). The Faculty of Science and the Graduate School, Chiang Mai University is also acknowledged. We would also like to thank the financial support from the Thailand Research Fund through the Royal Golden Jubilee Ph.D. Program. Authors also acknowledge the support of INAMM/NSF program at UTSA.

References

[1] P. Jaiban, A. Rachakom, S. Buntham, S. Jiansirisomboon, A. Watcharapasorn, Fabrication of $Bi_{0.5}Na_{0.5}ZrO_3$ powder by mixed oxide method, Materials Science Forum 695 (2011) 49–52.

[2] P. Jaiban, S. Jiansirisomboon, A. Watcharapasorn, Densification of $Bi_{0.5}Na_{0.5}ZrO_3$ ceramic using liquid-phase sintering method, Science Asia 37 (2011) 256–261.

[3] Lily, K. Kumari, K. Prasad, K.L. Yadav, Dielectric and impedance study of lead-free ceramic: $(Na_{0.5}Bi_{0.5})ZrO_3$, Journal of Materials Science 42 (2007) 6252–6259.

[4] P. Jaiban, A. Rachakom, S. Jiansirisomboon, A. Watcharapasorn, Influences of phase transition and microstructure on dielectric properties of $Bi_{0.5}Na_{0.5}Zr_{1-x}Ti_xO_3$ ceramics, Nanoscale Research Letters 7 (2012) 45.

[5] P. Jaiban, S. Jiansirisomboon, A. Watcharapasorn, Effect of lanthanum substitution on microstructure and electrical properties of $(Bi_{0.5}Na_{0.5})_{1-1.5x}La_xTi_{0.41}Zr_{0.59}O_3$ ceramics, Ceramics International 38 (2012) 379–383.

[6] D. Zhou, M. Kamlah, D. Munz, Effect of uniaxial prestress on the ferroelectric hysteretic response of soft PZT, Journal of the European Ceramic Society 25 (4) (2005) 425–432.

[7] R. Yimnirun, S. Ananta, A. Ngamjarurojana, S. Wongsaenmai, Uniaxial stress dependence of ferroelectric properties of xPMN–$(1-x)$PZT ceramic systems, Applied Physics A 81 (2005) 1227–1231.

[8] R.D. Shannon, Revised effective ionic radii and systematic studies of interatomic distances in halides and chalcogenides, Acta Crystallographica 32 (1976) 751–767.

[9] R.L. Holman, R.M. Fulrath, Intrinsic non-stoichiometry in the lead-zirconate lead–titanate system determined by Knudsen effusion, Journal of Applied Physics 44 (12) (1973) 5227–5236.

[10] A.I. Kingon, J.B. Clark, Sintering of PZT ceramics: I, atmosphere control, Journal of the American Ceramic Society 66 (4) (1983) 253–256.

[11] S.W. Zhang, H. Zhang, B.P. Zhang, S. Yang, Phase-transition behavior and piezoelectric properties of lead-free $(Ba_{0.95}Ca_{0.05})(Ti_{1-x}Zr_x)O_3$ ceramics, Journal of Alloys and Compounds 506 (2010) 131–135.

[12] D. Berlincourt, Piezoelectric crystals and ceramics, in: O.E. Mattiat (Ed.), Ultrasonic Transducer Materials, Plenum, London, 1971.

[13] R.S. Thomas, J.Z. Shujun, Lead-free piezoelectric ceramics: alternatives for PZT, Journal of Electroceramics 19 (2007) 111–124.

[14] R. Yimnirun, S. Ananta, E. Meechoowas, S. Wongsaenmai, Effects of uniaxial stress on dielectric properties leak magnesium niobate–lead zirconate titanate ceramics, Journal of Physics D 36 (2003) 1615–1619.